Chinese Journal of Natural Medicines

Therapeutic potential of alkaloid extract from Codonopsis Radix in alleviating hepatic lipid accumulation: insights into mitochondrial energy metabolism and endoplasmic reticulum stress regulation in NAFLD mice

Cailian FAN, Guan WANG, Miao CHEN, Yao LI, Xiyang TANG, Yi DAI

Citation: Cailian FAN, Guan WANG, Miao CHEN, Yao LI, Xiyang TANG, Yi DAI, Therapeutic potential of alkaloid extract from Codonopsis Radix in alleviating hepatic lipid accumulation: insights into mitochondrial energy metabolism and endoplasmic reticulum stress regulation in NAFLD mice, Chinese Journal of Natural Medicines, 2023, 21(6), 411−422. doi: 10.1016/S1875−5364(23)60403−0.

View online: https://doi.org/10.1016/S1875−5364(23)60403−0

Available online at www.sciencedirect.com
ScienceDirect
Chinese Journal of Natural Medicines 2023, **21**(6): 411-422
doi: 10.1016/S1875-5364(23)60403-0
Chinese Journal of Natural Medicines

•Original article•

Therapeutic potential of alkaloid extract from Codonopsis Radix in alleviating hepatic lipid accumulation: insights into mitochondrial energy metabolism and endoplasmic reticulum stress regulation in NAFLD mice

FAN Cailian[1], WANG Guan[2], CHEN Miao[3], LI Yao[3], TANG Xiyang[3*], DAI Yi[3]

[1] *College of Medicine, Henan Engineering Research Center of Funiu Mountain's Medicinal Resources Utilization and Molecular Medicine, Pingdingshan University, Pingdingshan 467000, China;*
[2] *Innovation Center of Nursing Research, Nursing Key Laboratory of Sichuan Province, West China Hospital, Sichuan University/West China School of Nursing, Sichuan University, Chengdu 610041, China;*
[3] *Guangdong Province Key Laboratory of Pharmacodynamic Constituents of TCM and New Drugs Research, College of Pharmacy, Jinan University, Guangzhou 510632, China*

Available online 20 Jun., 2023

[ABSTRACT] Alkaloids are a class of naturally occurring bioactive compounds that are widely distributed in various food sources and Traditional Chinese Medicine. This study aimed to investigate the therapeutic effects and underlying mechanisms of alkaloid extract from Codonopsis Radix (ACR) in ameliorating hepatic lipid accumulation in a mouse model of non-alcoholic fatty liver disease (NAFLD) induced by a high-fat diet (HFD). The results revealed that ACR treatment effectively mitigated the abnormal weight gain and hepatic injury associated with HFD. Furthermore, ACR ameliorated the dysregulated lipid metabolism in NAFLD mice, as evidenced by reductions in serum triglyceride, total cholesterol, and low-density lipoprotein levels, accompanied by a concomitant increase in the high-density lipoprotein level. ACR treatment also demonstrated a profound anti-oxidative effect, effectively alleviating HFD-induced oxidative stress and promoting ATP production. These effects were achieved through the up-regulation of the activities of mitochondrial electron transfer chain complexes I, II, IV, and V, in addition to the activation of the AMPK/PGC-1α pathway, suggesting that ACR exhibits therapeutic potential in alleviating the HFD-induced dysregulation of mitochondrial energy metabolism. Moreover, ACR administration mitigated HFD-induced endoplasmic reticulum (ER) stress and suppressed the overexpression of ubiquitin-specific protease 14 (USP14) in NAFLD mice. In summary, the present study provides compelling evidence supporting the hepatoprotective role of ACR in alleviating lipid deposition in NAFLD by improving energy metabolism and reducing oxidative stress and ER stress. These findings warrant further investigation and merit the development of ACR as a potential therapeutic agent for NAFLD.

[KEY WORDS] Codonopsis Radix; Alkaloids; Mitochondrial energy metabolism; Endoplasmic Reticulum stress; NAFLD
[CLC Number] R965 **[Document code]** A **[Article ID]** 2095-6975(2023)06-0411-12

Introduction

Non-alcoholic fatty liver disease (NAFLD) is a chronic metabolic disorder characterized by hepatic steatosis in the absence of excessive alcohol consumption [1]. There is an increasing body of evidence from the clinic that shows NAFLD is a key risk factor for the development of liver fibrosis, cirrhosis, and liver cancer [2, 3]. Despite years of extensive research into the pathogenesis of NAFLD, the lack of specific pharmacological interventions for NAFLD remains a critical challenge. Current clinical management of NAFLD predominantly revolves around lifestyle modifications, including weight loss, dietary control, exercise, and adjunctive pharmacotherapies encompassing lipid-lowering agents, hepatoprotective agent, and insulin sensitizers [4-7]. However, the use of these medications may entail undesirable side effects such as anorexia and headache [6]. Therefore, in-depth elucidation of the intricate mechanisms underlying NAFLD pathogenesis and the discovery of efficacious pharmacological interventions to halt or reverse disease progression are imperative for

[Received on] 29-Oct.-2022
[Research funding] This work was supported by the Scientific Research Foundation for the introduction of talent of Pingdingshan University (No. PXY-BSQD-2022040) and Guangdong Basic and Applied Basic Research Foundation (No. 2021A1515110055).
[*]**Corresponding author]** E-mails: tangxiyangjnu@163.com (TANG Xiyang)
These authors have no conflict of interest to declare.

advancing patient care in this context.

Emerging evidence highlights excessive lipid accumulation and heightened reactive oxygen species (ROS) levels as key contributors to the pathogenesis of NAFLD [8, 9]. ROS overproduction, a consequence of elevated oxidative stress, disrupts endogenous anti-oxidant defense mechanisms and induces liver cell injury [10, 11]. Clinical and experimental investigations have revealed that compromised anti-oxidant capacity not only impairs affects ATP production but also exacerbates mitochondrial energy metabolism dysfunction and insulin resistance, thereby promoting NAFLD progression [12, 13]. In addition, dysregulated lipid accumulation and elevated ROS levels induce perturbations in endoplasmic reticulum (ER) function [14]. Given its substantial metabolic activity in hepatocytes, the ER plays critical roles in protein synthesis, folding, modification, transport, as well as lipid and steroid hormone synthesis [15, 16]. Studies have confirmed the association between the accumulation of unfolded or misfolded proteins within the ER and the progression of NAFLD [17-19]. These aberrant proteins trigger the upregulation of molecular chaperones (*e.g.* BIP) and folding enzyme-related genes, initiating ER-associated protein degradation systems and inducing ER stress [19]. Prolonged ER stress further activates the protein kinase R-like ER kinase (PERK), activating transcription factor 6 (ATF6), and inositol-requiring enzyme 1 alpha (IRE1α) pathways, accelerating ROS generation and exacerbating disturbances in lipid metabolism [20]. Hence, targeted interventions aimed at mitigating oxidative stress and ER stress hold promise as effective strategies to improve hepatic steatosis in the development of NAFLD.

Alkaloids from food and herbal medicines are natural compounds known for their diverse biological activities, such as lipid-lowering and anti-insulin resistance properties [21, 22] Previous studies have demonstrated the efficacy of the total alkaloid extract from Lotus leaves (*Nelumbo nucifera* leaves) in reducing triglyceride (TG) and low-density lipoprotein (LDL) levels in experimental models of hypercholesterolemia [23]. Similarly, betaine, a constituent found in various vegetables and Traditional Chinese Medicine, has been shown to suppress fatty acid synthesis, enhance β-oxidation, and inhibit lipid transport, thereby alleviating lipid accumulation in high-fat diet (HFD) mice [24]. Therefore, alkaloids have emerged as promising candidates for the prevention and treatment of metabolic syndrome. Codonopsis Radix, a homolog of food and medicine, is widely used as an adjunct ingredient in culinary preparations to enhance immune function and nutrient absorption in China, Japan, and Singapore [25-27]. Modern pharmacological research has confirmed that Codonopsis Radix has neuroprotective, anti-tumor, anti-oxidant, anti-inflammatory, anti-stress, and hepatoprotective activitives [28-33]. Chemical analysis of Codonopsis Radix has revealed that its principal constituents mainly include alkaloids, alkynes, flavonoids, and saccharides [32, 34, 35]. While prior studies have primarily focused on the pharmacological activities of total flavonoids, alkynes, and saccharidesderived from ACR, limited research has explored the therapeutic effects and underlying mechanisms of action of alkaloids from Codonopsis Radix (ACR) in ameliorating lipid accumulation. Therefore, our research team endeavored to investigate the effects and potential mechanisms of ACR mitigating lipid accumulation in HFD-induced NAFLD mice.

Materials and Methods

Materials and reagents

Fenofibrate (FENO, HY-17356B) was obtained from MedChemExpress (USA). The primary antibodies against β-Actin (AF7018), PERK (AF5304), phosphorylated (p)-PERK (DF7576), USP14 (DF9982), C/EBP-homologous protein (Chop, DF6025), and the secondary antibody against rabbit (S0001) were obtained from Affinity Biosciences (Jiangsu, China). The primary antibodies against p-eukaryotic initiation factor-2 alpha (p-eIF2α, AF1237), eIF2α (AF1237), p-IRE1α (AF5842), IRE1α (AI601), ATF6 (AF6243) and glucose-regulated protein 78 (GRP78, AF0171) were purchased from Beyotime Biotechnology (Shanghai, China). The antibodies against p-AMPK (4184), AMPK (2532) and PGC-1α (2178) were purchased from Cell Signaling Technology (Denver, USA). The ECL system for Western blotting substrate detection was obtained from Biosharp (Anhui, China). Formic acid was obtained from Sigma-Aldrich (MO, USA), and dichloromethane and ethanol were obtained from Damao Chemical Reagent Factory (Tianjin, China). Water and acetonitrile were purchased from Fisher Scientific (NJ, USA).

Plant material and preparation of ACR

Codonopsis Radix (A20191020) was provided and identified by Guangdong Tai'antang Pharmaceutical Co., Ltd. (Guangzhou, China). The dried herbal material of Codonopsis Radix (1.0 kg) was soaked overnight in 70% ethanol, followed by two cycles of heating and refluxing, each lasting two hours. Then the extract of Codonopsis Radix (176.3 g) was further concentrated. Next, the ethanol extract was dissolved in water and subjected to three successive extractions using petroleum ether and dichloromethane. The resulting dichloromethane fraction, rich in alkaloids, was concentrated to yield ACR (4.6 g). The obtained extract was collected and stored at −20 °C until further use.

Identification and quantification of alkaloid compounds of ACR using ultra performance liquid chromatography-quadrupole time-of-flight/mass spectrometry (UPLC-Q-TOF/MS)

A total of 3.0 mg of ACR was meticulously weighed and transferred into a 15 mL centrifuge tube. To prepare the ACR solution for analysis, 3 mL of a 60% methanol-water solution was added, resulting in a concentration of 1 mg·mL^{-1}. The supernatant containing ACR was obtained by subjecting the mixture to centrifugation at 14 000 r·min^{-1} for 15 min. The identification and quantification of alkaloid compounds in ACR were performed using UPLC-Q-TOF/MS. The separation of alkaloids in ACR was achieved using an AC-

QUITY™ ultra-performance LC system (Waters, USA) equipped with a chromatographic column (ACQUITY UPLC BEH C_{18}, 2.1 mm × 100 mm, 1.7 μm, Waters, USA). MS was conducted on a SYNAPT™ G2 mass spectrometer (Waters, UK). Table S1 provides a comprehensive description of the liquid chromatography and MS conditions.

Animal grouping and feeding

This study was conducted in accordance with guidelines and regulations set forth by the Ethics Committee for Experimental Animals of West China Hospital of Sichuan University (Approval No. 20211127A). A total of 40 male mice, aged 6 weeks and weighing 18 ± 5 g (Beijing HFK Bioscience Co., Ltd., Beijing, China) were housed in groups (n = 4/cage), maintained under a controlled 12-h light/dark cycle, and provided with unrestricted access to rodent chow and water for a week to allow for acclimatization to the laboratory environment.

Following an initial week of acclimatization on a standard diet, the 40 mice were randomly allocated into five groups as follows: (1) Normal-fat diet (NFD) group, receiving a NFD for 12 weeks; (2) HFD group, receiving a HFD for 12 weeks; (3) HFD + high-dose ACR (H-ACR) group, receiving a daily intragastric administration of 150 mg·kg^{-1}·d^{-1}. ACR in conjunction with a HFD for 12 weeks; (4) HFD + low-dose ACR (L-ACR), receiving a daily intragastric administration of 50 mg·kg^{-1}·d^{-1} ACR in conjunction with a HFD for 12 weeks; (5) HFD + FENO group, receiving a daily intragastric administration of 100 mg·kg^{-1}·d^{-1} FENO in conjunction with a HFD for 12 weeks. The doses of ACR used in this study were determined based on the preliminary experiment results. The HFD was prepared in-house by our research team using a formulation comprising 60% ordinary rodent feed, 5% sucrose, 10% lard, 5% whole milk powder, 15% yolk, 3% cholesterol, and 2% salt. All dietary components were sterilized by UV irradiation. The body weights of all mice were measured and recorded weekly throughout the experimental period.

Serum analysis and biochemical parameter evaluation

At the end of 12-week experimental period, eyeballs were collected from all mice to obtain blood samples. The blood samples were then centrifuged at 4 000 r·min^{-1} for 15 min to separate the serum for subsequent analysis. The levels of serum alanine aminotransferase (ALT) and aspartate aminotransferase (AST) were detected using an automated biochemical analyzer (Thermo Fisher Scientific, USA). In addition, the levels of serum total cholesterol (TC), TG, high-density lipoprotein (HDL), and LDL were measured using assay kits (Applygen, Beijing, China).

Analysis of oxidative stress indices in the liver

The activities of malondialdehyde (MDA), superoxide dismutase (SOD), and reduced glutathione (GSH) in liver tissues were detected using the kits from Nanjing Jiancheng Bioengineering Institute (Nanjing, China). Briefly, 0.5 g of liver samples were homogenized in 3 mL of cold phosphate buffer, followed by centrifugation at 13 000 r·min^{-1} for 15 min at 4 °C to obtain supernatants. Before the determination of lipid peroxidation, the protein concentrations in the liver tissue homogenates were measured using the BCA Protein Assay Kit (Beyotime Biotechnology, Shanghai, China). The activities of MDA, SOD and GSH in liver tissues were measured at 530 nm, 450 nm, and 410 nm, respectively, using a microplate reader (BioTek Instruments Inc., USA).

Histopathological examination

Histopathological examination using hematoxylin and eosin (H&E) staining was performed to assess the histopathological alterations in the liver tissues of the mice. In addition, hepatic neutral lipid deposition was visualized using Oil Red O staining. The specific protocols for H&E and Oil-red O staining were performed according to established procedures, as described previously [36].

Analysis of ATP production

ATP production was evaluated using an ATP Analysis Kit (Beyotime Biotechnology). In brief, liver tissue samples weighing approximately 50 mg were homogenized and then centrifuged at 13 000 r·min^{-1} for 5 min to obtain the supernatant. The supernatant was then subjected to detection of emitted light using a microplate photometer (BioTek Instruments Inc.) after the addition of various dilutions of luciferase reagent.

Isolation of liver mitochondria

Following approved euthanasia procedures, fresh liver samples were promptly collected from the experimental subjects for liver mitochondria isolation using the Tissue Mitochondria Isolation Kit (Beyotime Biotechnology), following established protocols [37, 38]. Briefly, 100 mg of fresh liver samples were incubated with 1 mL of pre-cooled mitochondrial separation reagent A and homogenized in an ice bath 10 cycles. Next, the homogenates were centrifuged at 4 ºC, 800 r·min^{-1} for 5 min. Subsequently, the supernatants were carefully transferred to a new 1.5 mL EP tube for centrifugation at 4 ºC, 12 000 r·min^{-1} for 10 min. Then the supernatants were removed, and the resulting pellet was gently resuspended in phosphate-buffered saline (PBS). The protein concentrations of the liver mitochondria were determined using the BCA Protein Assay Kit.

Analysis of respiratory chain complexes I−V activities

The activities of mitochondrial respiratory chain complexes I–V were detected by Complexes I–V Assay kits (Solarbio, Beijing, China). Briefly, liver mitochondria were isolated and appropriately diluted with PBS. Subsequently, the diluted mitochondria were subjected to enzymatic assays following the manufacturer's instructions. The activities of complexes I–V were spectrophotometrically measured at specific wavelengths (I: 340 nm, II: 600 nm, III: 500 nm, IV: 550 nm, V: 660 nm) using a microplate reader (BioTek Instruments).

Quantitative real-time PCR (qRT-PCR)

The mRNA expression levels of *Fasn*, *Fabp1*, *Scd1*, and *Actin* in liver tissues were detected by qRT-PCR. Total RNA was extracted from the liver tissues using an RNA extraction reagent (Servicebio, Wuhan, China) according to the manu-

facturer's instructions. Subsequently, the isolated RNA was reversely transcribed into cDNA using the RevertAid First Strand cDNA Synthesis Kit (Servicebio). The primer sequences specific to the target genes (*Fasn*, *Fabp1*, *Scd1*, and *Actin*) for qRT-PCR were designed by Tsingke Biotechnology Co., Ltd. (Beijing, China) for PCR amplification. The expression levels of the target genes were normalized to the reference gene *Actin* to account for variations in RNA input and reverse transcription efficiency.

Western blotting analysis

The protein expression levels of p-IRE1α, ATF6, IRE1α, GRP78, p-AMPK, AMPK, PGC-1α, p-PERK, USP14, PERK, p-eIF2α, Chop, eIF2α and β-Actin in the liver samples were assessed using Western blotting analysis, following a previously established protocol [37]. The specific dilution ratios for each primary antibody were as follows: p-IRE1α (1 : 1000), IRE1α (1 : 1000), ATF6 (1 : 1000), GRP78 (1 : 1000), p-AMPK (1 : 800), AMPK (1 : 1000), PGC-1α (1 : 1000), p-PERK (1 : 1000), PERK (1 : 1000), USP14 (1 : 1000), p-eIF2α (1 : 700), eIF2α (1 : 700), Chop (1 : 1000), and β-Actin (1 : 4000). The Western blotting results were independently validated through three repeated experiments.

Statistical analysis

All statistical analyses in this study were performed using GraphPad Prism software (version 7.0) through one-way analysis of variance (ANOVA). The data were presented as the mean ± SD. $P < 0.05$ was indicative of a statistically significant difference between different groups.

Results

Phytochemical compositions of ACR were analyzed by UPLC-Q-TOF/MS

The phytochemical profile of ACR was investigated by UPLC-Q-TOF/MS in this study (Fig. 1). Through comparison of the retention times and MS/MS fragment ions with standards, a total of 9 alkaloid compounds were identified (Table 1, Fig.S1).

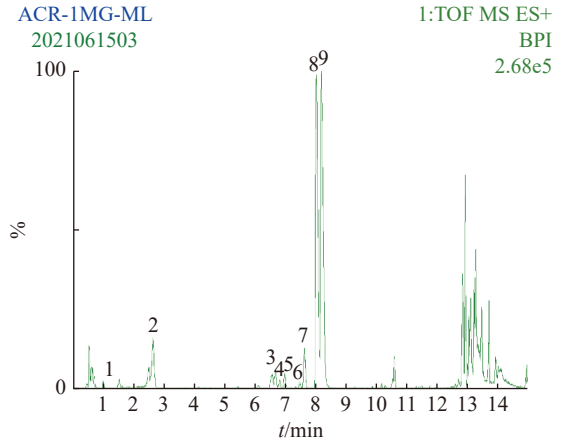

Fig. 1 Characterization of the main compounds of ACR by UPLC-Q-TOF/MS in positive-ion mode. (1) codonopyrrolidium B; (2) codonopyrrolidium I; (3) codonopyrrolidium H; (4) codonopyrrolidium A; (5) codonopyrrolidium F; (6) codonopyrrolidium C; (7) codonopyrrolidium G; (8) codonopyrrolidium D; (9) codonopyrrolidium E.

ACR treatment improved HFD-induced hepatic injury and associated body weight gain

The impact of a long-term HFD on fat intake, blood lipid levels, and subsequent development of liver steatosis has been well-documented [39]. Therefore, HFD-fed mice or rats have been widely employed as a classical model to assess the therapeutic efficacy of anti-NAFLD drugs. As shown in Figs. 2A−2B, the HFD group exhibited significantly increased body weight, liver weight, and food intake compared with those in the NFD group, while the administration of 150 $mg \cdot kg^{-1}$ ACR (H-ACR) and 100 $mg \cdot kg^{-1}$ FENO (positive drug group) remarkably reduced the body and liver weight in mice ($P < 0.01$). In addition, H-ACR and FENO groups showed a decrease in food intake compared with the HFD group, was although no statistically significant difference was observed between them (Fig. 2C, $P > 0.05$).

To further ascertain the impact of ACR on liver function in NAFLD mice, the serum activities of ALT and AST were

Table 1 Characterization of the main compounds of ACR by UPLC-Q-TOF/MS

No.	$t_R$min	Compounds	Selected ion	Formula	Detected	Mass error (mDa)	MS fragments
1	1.03	codonopyrrolidium B	$[M]^+$	$C_{14}H_{22}NO_4$	268.1547	−0.2	250.1422, 161.0601, 121.0655, 88.0755
2	2.64	codonopyrrolidium I	$[M]^+$	$C_{19}H_{28}NO_6$	366.1916	−0.1	266.1392, 177.0549, 161.0592, 137.0590, 88.0744
3	6.68	codonopyrrolidium H	$[M]^+$	$C_{19}H_{30}NO_6$	368.2062	0.5	266.1391, 220.1389,202.1451, 172.1351, 121.0667, 100.0762, 88.0767
4	6.82	codonopyrrolidium A	$[M]^+$	$C_{19}H_{28}NO_5$	350.1967	0	268.1535, 250.1436, 220.1324, 161.0637, 121.0647, 88.0750
5	7.01	codonopyrrolidium F	$[M]^+$	$C_{19}H_{30}NO_5$	352.2126	0.2	250.0865, 161.0609, 121.0660, 88.0750
6	7.49	codonopyrrolidium C	$[M]^+$	$C_{19}H_{28}NO_5$	350.1974	0.7	250.1452, 232.1339,170.1187, 161.0603, 121.0649
7	7.64	codonopyrrolidium G	$[M]^+$	$C_{19}H_{30}NO_5$	352.2119	0.5	250.1430, 161.0606, 121.0658, 88.0768
8	8.07	codonopyrrolidium D	$[M]^+$	$C_{19}H_{30}NO_5$	352.2119	−0.5	250.1460, 232.1308, 172.1327, 121.0667, 88.0758
9	8.24	codonopyrrolidium E	$[M]^+$	$C_{19}H_{30}NO_5$	352.2121	−0.3	250.1460, 232.1274, 172.1351, 121.0667, 88.0754

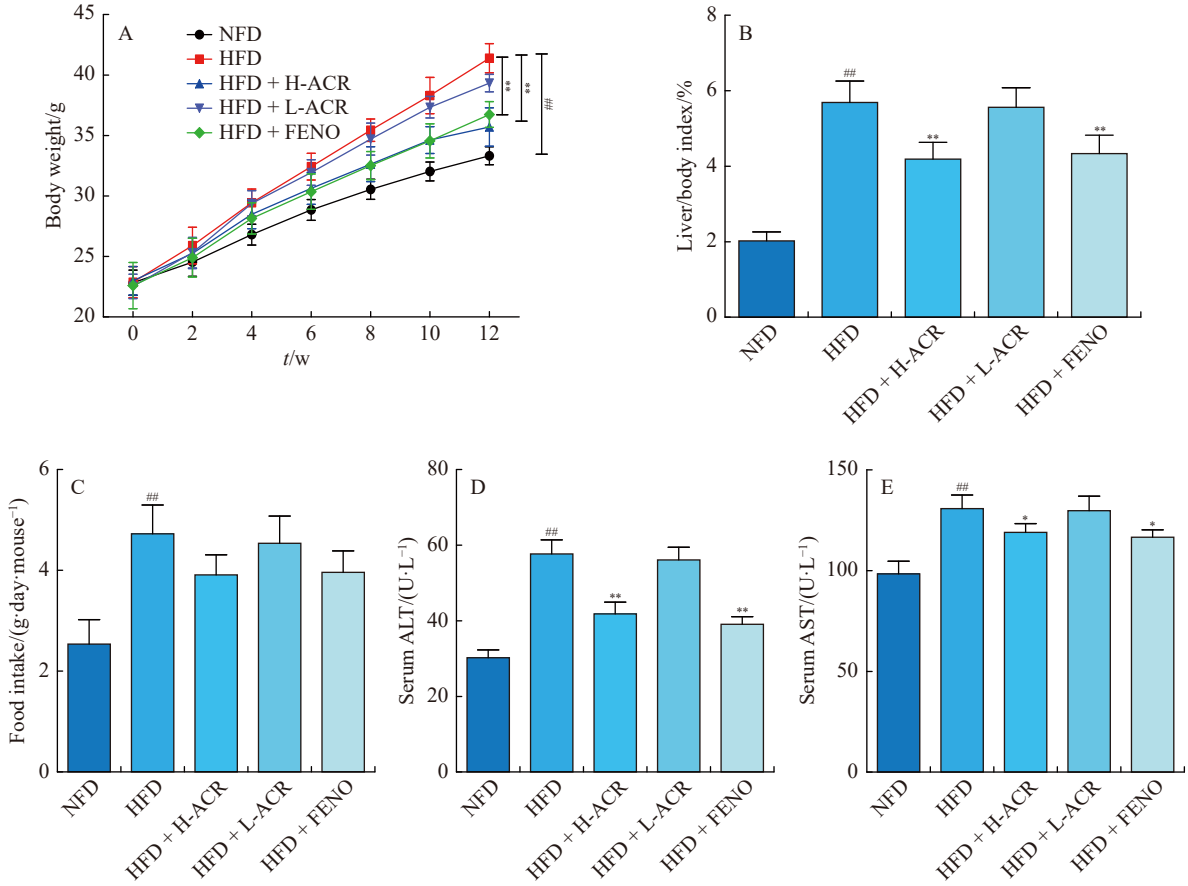

Fig. 2 ACR attenuated HFD-induced body weight gain and liver injury in NAFLD mice. (A) Changes of body weight were recorded during ACR treatment in the progression of NAFLD. (B) The index of liver/body in HFD-fed mice treated with ACR (50 mg·kg^{-1}·d^{-1} and 150 mg·kg^{-1}·d^{-1}) or FENO (100 mg·kg^{-1}·d^{-1}) for 12 weeks were counted. (C) The food intake (g/day/mouse) in different groups was recorded. (D–E) Levels of serum ALT and AST in different groups were detected using Automatic biochemical analyzer. The data were expressed as mean ± SD; (n = 8). $^{\#\#}$ P < 0.01 *vs* NFD group; * P < 0.05, ** P < 0.01 *vs* HFD group.

determined. As depicted in Fig. 2D and Fig. 2E, the activities of serum ALT and AST exhibited a substantial up-regulation in the HFD group compared with those in the NFD group (P < 0.01), whereas treatment with 150 mg·kg^{-1} ACR (H-ACR) and 100 mg·kg^{-1} FENO treatment led to a significant down-regulation of ALT and AST activities (P < 0.05). Remarkably, the effect of ACR in mitigating body weight gain and reducing ALT and AST activities in the serum closely paralleled that of FENO, suggesting that ACR can attenuate HFD-induced hepatic injury and associated weight gain.

ACR could alleviate HFD-induced hepatic steatosis and regulate HFD-induced glucose and lipid metabolism disorders

NAFLD, characterized by hepatic lipid accumulation, is a chronic disease with significant implications [40]. In this study, we investigated the effects of ACR on HFD-induced hepatic steatosis and the level of insulin. Histopathological examination using H&E and Oil Red O staining revealed pronounced diffuse bullous steatosis and hepatocyte swelling in the liver of mice in the HFD group (Fig. 3A and Fig. 3B), suggesting that the long-term HFD causes hepatic steatosis. However, treatment with 150 mg·kg^{-1} ACR (H-ACR) and 100 mg·kg^{-1} FENO resulted in a noticeable reduction in HFD-induced lipid deposition. Consistent with these pathological changes, the HFD group exhibited significantly elevated levels of serum glucose, insulin, TC, TG, and LDL (P < 0.01, Fig. 3C–Fig. 3G), accompanied by a marked reduction in the level of HDL (P < 0.01, Fig. 3H). Furthermore, qRT-PCR analysis (Fig. 3I–Fig. 3K) demonstrated that mRNA expression levels of key genes involved in fatty acid uptake and synthesis related genes (*Fasn*, *Fabp1* and *Scd1*) were markedly upregulated in response to long-term HFD treatment. Importantly, treatment with ACR and FENO effectively reversed these alterations induced by a HFD (Fig. 3C–Fig. 3K, Table 2), highlighting the potential of ACR to ameliorate HFD-induced disturbances in glucose and lipid metabolism. Collectively, these findings establish the beneficial role of ACR in alleviating HFD-induced hepatic steatosis and restoring HFD-induced glucose and lipid homeostasis.

ACR ameliorated HFD-induced oxidative injury in NAFLD mice

Considering the well-established association between the development of NAFLD and the persistent occurrence of oxidative stress, we evaluated the effect of ACR on HFD-induced liver oxidative injury by assessing the activities of liv-

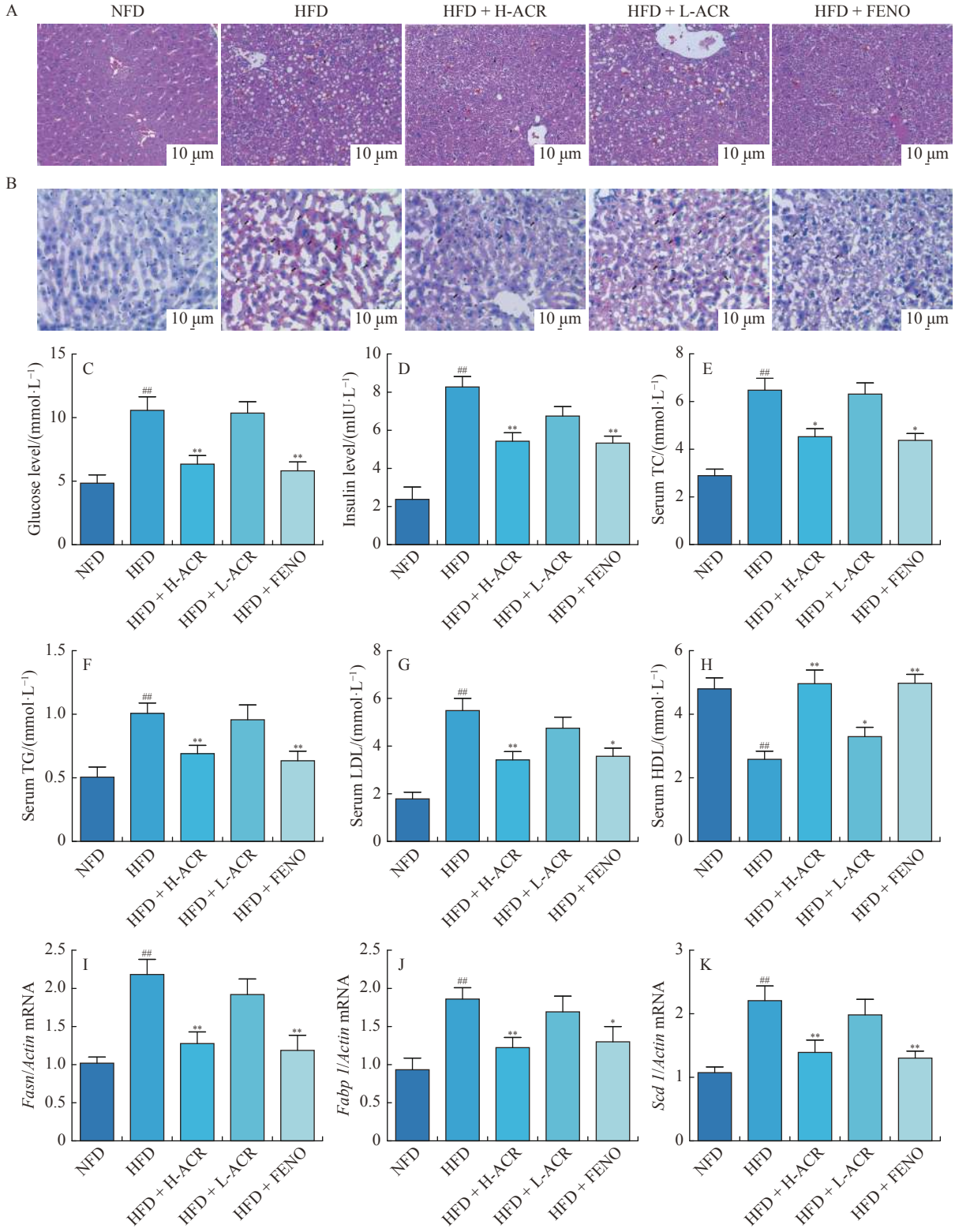

Fig. 3 ACR improved HFD-induced glucose and lipid metabolism disorder in NAFLD mice. (A, B) Representative images of H&E and Oil red O staining of liver tissue; scale bar 10 μm. Fat vacuoles: red arrow; Ballooning degeneration: black filled triangle; Fatty degeneration: black filled arrow. (C−H) Levels of serum blood glucose (C), insulin (D), TC (E), TG (F), LDL (G) and HDL (H) in NAFLD mice were detected. (I−K) The mRNA levels of *Fasn* (I) , *Fabp 1* (J) , and *Scd 1* (K) genes in mice. Gene expression was normalized to Actin mRNA levels. The data were expressed as mean ± SD; (n = 8). $^{\#\#}P < 0.01$ *vs* NFD group; $^{*}P < 0.05$, $^{**}P < 0.01$ *vs* HFD group.

Table 2 ACR improved liver and serum metabolic parameter levels in HFD mice (means ± SD, n = 8)

Group	NFD	HFD	HFD + H-ACR	HFD + L-ACR	HFD + FENO
liver TG (μg·mL^{-1})	38.23 ± 2.56	76.26 ± 4.49$^{\#\#}$	56.36 ± 4.10**	75.50 ± 3.22	53.34 ± 3.03**
Serum TC (mmol·L^{-1})	2.89 ± 0.27	6.48 ± 0.50$^{\#\#}$	4.53 ± 0.34**	6.31 ± 0.47	4.38 ± 0.29
Serum TG (mmol·L^{-1})	0.51 ± 0.08	1.01 ± 0.08$^{\#\#}$	0.69 ± 0.07**	0.96 ± 0.12	0.64 ± 0.08**
HDL (mmol·L^{-1})	4.80 ± 0.35	2.58 ± 0.26$^{\#\#}$	4.96 ± 0.43**	3.30 ± 0.29*	4.98 ± 0.28**
LDL (mmol·L^{-1})	1.79 ± 0.28	5.49 ± 0.51$^{\#\#}$	3.42 ± 0.35**	4.75 ± 0.46	3.58 ± 0.34*
VLDL (mmol·L^{-1})	2.60 ± 0.60	7.46 ± 0.53$^{\#\#}$	5.20 ± 0.48*	6.46 ± 0.44	4.65 ± 0.41**

$^{\#}P < 0.05$ and $^{\#\#}P < 0.01$ *vs* NFD group; $^{*}P < 0.05$ and $^{**}P < 0.01$ *vs* HFD group

er MDA, GSH, and SOD [8]. As displayed in Fig. 4A and Fig. 4B, the HFD group exhibited significant reductions in SOD and GSH activities in liver tissues compared with the NFD group ($P < 0.01$), while treatment with both H-ACR and FENO effectively prevented the decline in enzymatic activities, restoring them to levels similar to the NFD group ($P < 0.01$). Notably, HFD + L-ACR group also showed a trend towards restored SOD and GSH activities, although the difference did not reach statistical significance. Moreover, the level of MDA, a marker of oxidative stress, was significantly increased in the HFD group, indicating liver oxidative injury ($P < 0.01$). Remarkably, both HFD + H-ACR and FENO groups exhibited a significant reduction in MDA levels compared with the HFD group ($P < 0.01$), but no significant difference was observed between HFD + H-ACR group and HFD + FENO group ($P < 0.01$, Fig. 4C). Moreover, there was no significant difference between groups ACR and FENO on the improvement of these changes. Above results suggested that ACR administration could alleviate HFD-induced oxidative stress by enhancing the antioxidant system.

ACR administration could improve HFD-induced mitochondrial energy anomaly by regulation of AMPK/PGC-1α pathway

In the pathogenesis of NAFLD, the excessive consumption of HFD leads to mitochondrial dysfunction in hepatocytes, characterized by increased ROS production and impaired energy metabolism [13, 14]. Therefore, the effects of ACR on mitochondrial energy metabolism in NAFLD mice were evaluated in this study. As shown in Table 3 and Fig. 5A-Fig. 5F, the HFD group exhibited a significant decrease in ATP content and activities of mitochondrial respiratory chain complexes I–V ($P < 0.01$, $P < 0.05$), while the ATP production and activities of complex I, II, IV and V in the ACR and FNEO groups were increased ($P < 0.05$). In contrast, treatment with ACR and FENO resulted in increased ATP production and enhanced activities of complexes I, II, IV, and V ($P < 0.05$), albeit still lower than those in the control group. Notably, the increase in complex III following ACR and FENO treatment was not statistically significant compared to the HFD group ($P > 0.05$, Fig. 5D).

In addition, we investigated the signaling pathways associated with energy metabolism. AMPK, a key cellular energy sensor, has emerged as a potential therapeutic target for metabolic disorders [41, 42]. Mounting evidence indicates that mitochondrial status can influence AMPK activity, and in turn, AMPK regulates the function of mitochondria in many ways [41]. As depicted in Fig. 5G-Fig. 5I, the levels of PGC-1α/Actin and p-AMPK/AMPK ratios were significantly reduced by approximately 50% following HFD treatment. However, administration of 150 mg·kg^{-1} ACR and FENO markedly upregulated the levels of PGC-1α/Actin and p-AMPK/AMPK ratios ($P < 0.05$). These findings suggest that

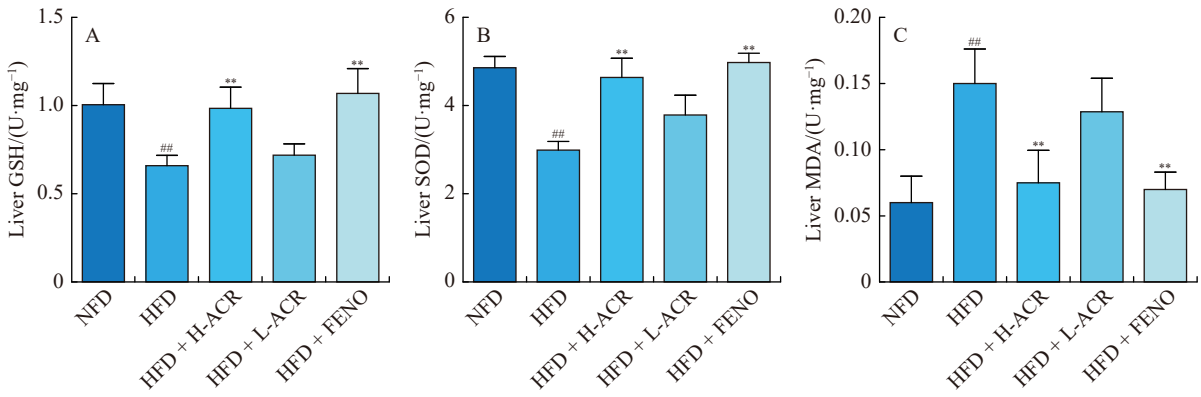

Fig. 4 ACR attenuated HFD-induced oxidative stress in mice. (A–C) The activities of SOD (A), GSH (B), and MDA (C) were measured with commercial kits in different groups. The data are expressed as mean ± SD; n = 8. $^{\#\#}p < 0.01$ *vs* NFD group; $^{**}p < 0.01$ *vs* HFD group.

Table 3 ACR regulated HFD-induced mitochondrial energy metabolism in mice (means ± SD, *n* = 8)

Group	NFD	HFD	HFD + H-ACR	HFD + L-ACR	HFD + FENO
ATP content (nmol·mg^{-1} prot)	64.40 ± 5.77	40.58 ± 3.68$^{\#\#}$	59.69 ± 6.39*	49.89 ± 5.24	61.71 ± 3.92**
Complex I activity(U·mg^{-1} prot)	15.65 ± 1.24	8.64 ± 1.61$^{\#\#}$	12.68 ± 1.04*	10.36 ± 1.24	12.79 ± 1.54*
Complex II activity (U·mg^{-1} prot)	10.28 ± 1.47	5.21 ± 1.07$^{\#\#}$	8.69 ± 1.20*	6.14 ± 1.23	9.23 ± 1.47**
Complex III activity (U·mg^{-1} prot)	3.29 ± 0.81	2.15 ± 0.50$^{\#}$	2.64 ± 0.60	2.45 ± 0.54	2.70 ± 0.58
Complex IV activity (U·mg^{-1} prot)	2.41 ± 0.49	1.58 ± 0.31$^{\#\#}$	2.31 ± 0.35*	1.96 ± 0.24	2.34 ± 0.42*
Complex V activity (U·mg^{-1} prot)	2.26 ± 0.34	1.48 ± 0.37$^{\#\#}$	2.15 ± 0.39*	1.73 ± 0.29	2.20 ± 0.38*

$^{\#}P < 0.05$ and $^{\#\#}P < 0.01$ *vs* NFD group; $^{*}P < 0.05$ and $^{**}P < 0.01$ *vs* HFD group

ACR treatment can ameliorate HFD-induced mitochondrial energy disturbances, potentially through activation of the AMPK/PGC-1α pathway.

ACR inhibited HFD-induced ER stress in NAFLD mice

Previous studies have established the involvement of ER stress in the pathogenesis of NAFLD, highlighting the up-regulation of USP14, a key player in lipid aggregation, as a consequence of sustained ER stress [43, 44]. Therefore, we sought to investigate the impact of ACR on ER stress-related signaling pathways and USP14 expression in HFD-induced NAFLD mice using Western blot assays. As illustrated in Fig.6A-Fig.6H, the ratios of p-PERK/PERK, p-IRE1α/IRE1α, ATF6/Actin, GRP78/Actin, p-eIF2α/eIF2α, and Chop/Actin, representing canonical ER stress signaling pathways, along with the expression of USP14, exhibited a minimum 1.5-fold increase upon HFD feeding. The positive control drug showed a similar effect to ACR in regulating the expressions of ER stress proteins and USP14, except for the expression of ATF6. The above data indicated that ACR could inhibit ER stress in HFD-induced NAFLD, which may be related to the expression of USP14.

Discussion

Alkaloids, a class of naturally occurring compounds with diverse biological activities, are widely distributed in nature [22]. Codonopsis Radix, a prominent Traditional Chinese Medicinal herb, is known for its high alkaloid content. In this study, the effects and underlying mechanisms of ACR in ameliorating lipid accumulation in a mouse model of HFD-induced NAFLD were investigated. Our findings provide compelling evidence for the ability of ACR to mitigate hepatic lipid deposition in NAFLD mice by enhancing energy metabolism, mitigating oxidative stress, and alleviating ER stress.

Numerous scientific investigations have consistently highlighted hepatic steatosis as the primary pathogenic mechanism underlying NAFLD [45]. Therefore, the widely employed approach of feeding mice a HFD for a duration of 8–12 weeks has been established as a reliable method for establishing an *in vivo* NAFLD model [46, 47]. During the HFD feeding regimen, mice exhibit increased liver index and serum levels of ALT, GLU, TC, TG and LDL, alongside decreased serum HDL levels. Furthermore, the liver presents varying degrees of steatosis, accompanied by inflammatory cell infiltration and other pathological changes [46, 47]. In our study, a mouse model of NAFLD was successfully constructed following 12 weeks of HFD treatment, as evidenced by the observed increase in body weight, liver weight relative to body weight index, and serum AST and ALT levels. These findings were consistent with histological analysis using H&E and Oil Red O staining, as well as measurements of TC, TG, LDL, and HDL levels in the serum were further confirmed, corroborating existing literature reports [46]. Treatment with ACR significantly attenuated weight gain and reduced serum ALT and AST levels in NAFLD mice. Furthermore, ACR intervention led to notable reductions in intracellular lipid deposition in the livers of HFD-induced mice and lowered serum levels of TC, TG, and LDL. Notably, these effects on lipid accumulation were comparable to those observed with the positive control drug FENO, unequivocally demonstrating the potent lipid-regulating properties of ACR in NAFLD.

Oxidative stress and lipid peroxidation, as the core of the "second strike", are indispensable in the occurrence and development of NAFLD [45]. Oxidative stress primarily arises from the the excessive production of ROS [11]. When the clearance of ROS fails to keep pace with their production it leads to lipid and protein peroxidation within mitochondria. Subsequently, the opening of mitochondrial membrane permeability transition pores is triggered, resulting in a decline or complete loss of mitochondrial membrane potential, disruption of mitochondrial structure, and impairment of mitochondrial function [11, 37]. In line with these reports, our study demonstrated that ACR alleviated HFD-induced oxidative stress injury, as evidenced by a reduction in the level of MDA and elevations in GSH and SOD activities. These data indicate that the lipid-lowering effects of ACR in NAFLD mice may, in part, be attributed to its potent anti-oxidative effect.

Mitochondria serve as the primary source of ROS production and ATP synthesis [48]. ATP generation within mitochondria is primarily accomplished through the coordinated functioning of the five respiratory chain complexes, namely complexes I–V, located on the inner mitochondrial membrane [49]. The key role of mitochondrial respiratory chain

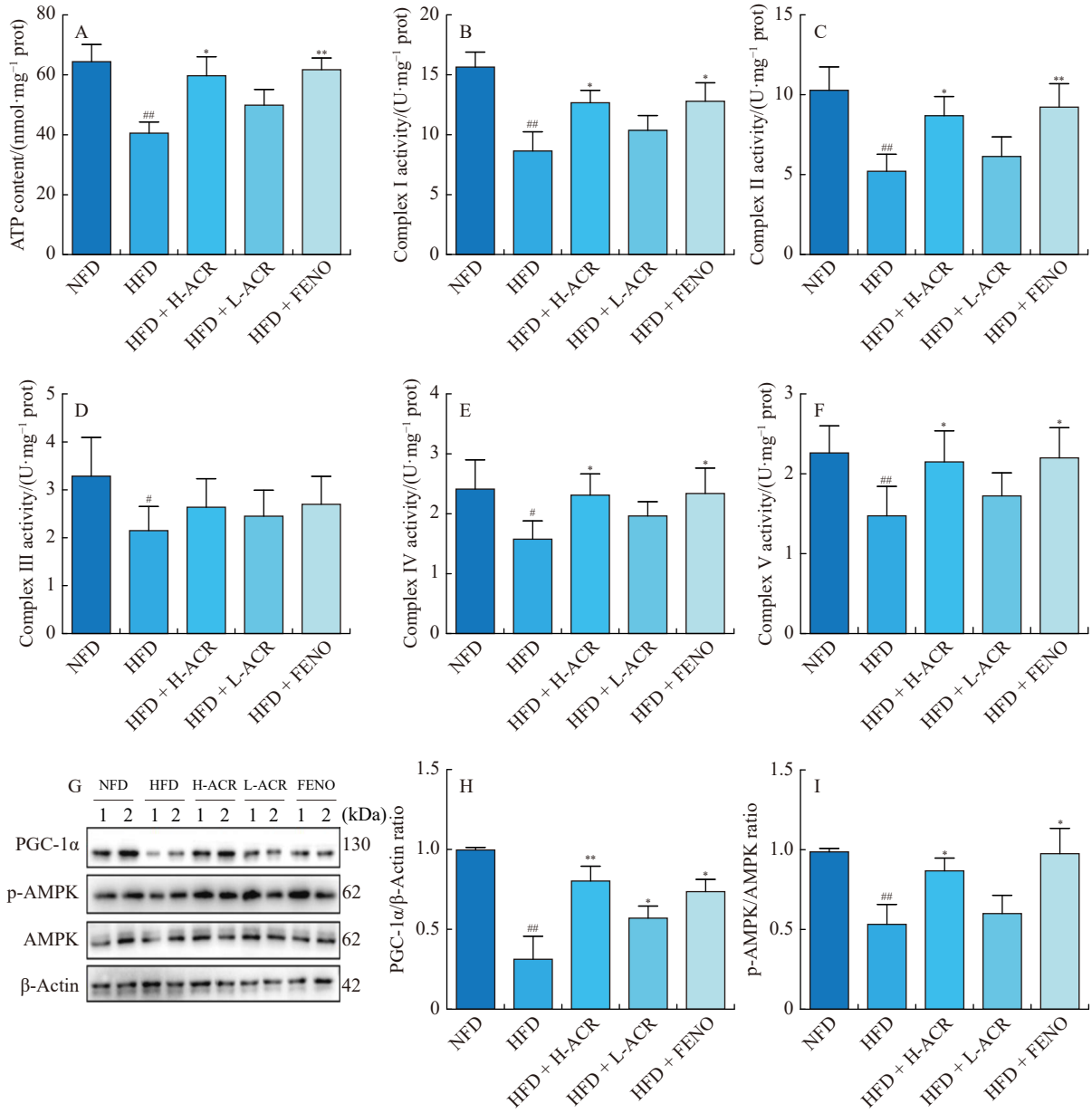

Fig. 5 ACR regulated HFD-induced mitochondrial energy metabolism disorder in mice. (A) Effect of ACR and FENO on ATP content in liver of mice was evaluated by a commercial kit. (B−F) Effects of ACR and FENO on the activities of Complex I (B), Complex II (C), Complex III (D), Complex IV (E) and Complex V (F) were detected by Elisa kits in liver of mice. (G) The protein expressions of p -AMPK, AMPK, PGC-1α and Actin were recorded by Western blotting bands. (H, I) Relative protein levels of p -AMPK/AMPK and PGC-1α/Actin in different groups were measured by Image J. The data were expressed as mean ± SD; $n = 4$. $^{\#\#}P < 0.01$ *vs* NFD group; $^{*}P < 0.05$, $^{**}P < 0.01$ *vs* HFD group.

complex enzymes is to release energy through a series of redox reactions during electron transfer, and finally synthesize ATP to provide energy for hepatocytes [49]. Heightened ROS production impairs the function of the mitochondrial respiratory chain, resulting in diminished ATP synthesis, perturbed hepatic metabolic function, and subsequent hepatic steatosis [49, 50]. Therefore, the integrity of the mitochondrial respiratory chain is a prerequisite for ensuring normal liver function. In our study, the ATP production and activities of mitochondrial respiratory chain complexes (I–V) were obviously reduced in HFD-fed mice, indicating that HFD causes abnormal mitochondrial energy metabolism. After ACR intervention, the ATP production in mitochondria and the activities of mitochondrial respiratory chain complexes (I, II, IV and V) were obviously enhanced. However, it is important to note that although the activity of mitochondrial respiratory chain complex III was up-regulated by ACR treatment, the difference was not statistically significant.

It is well recognized that the change of ATP content in cells will affect the activation of AMPK [50]. AMPK, a member of the serine protein kinase family, which plays an important role in maintaining energy metabolism homeostasis [51].

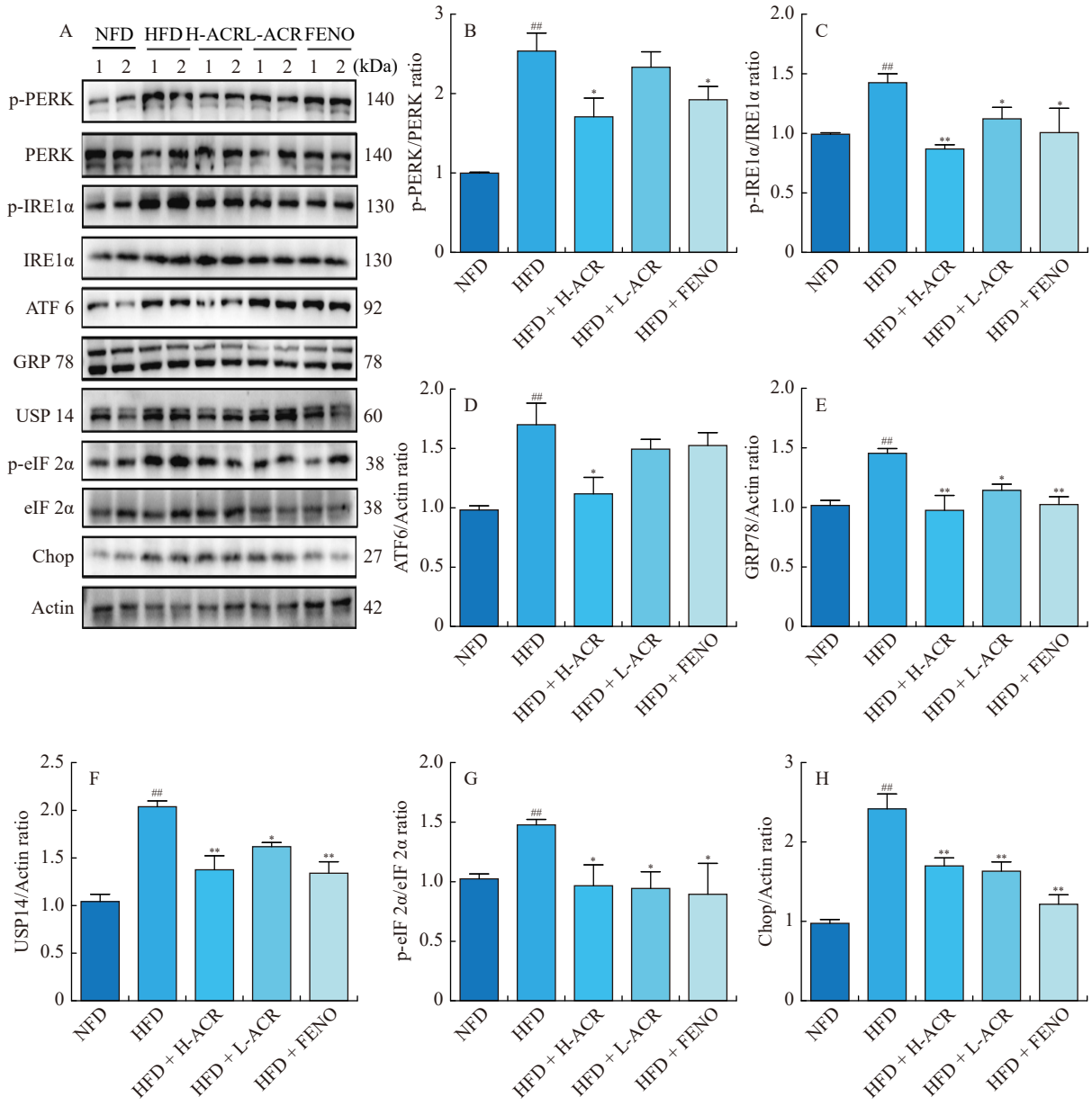

Fig. 6 ACR alleviated HFD-induced ER stress in NAFLD mice. (A) The protein expressions of p-PERK, PERK, p-IRE1α, IRE1α, ATF 6, GRP 78, USP14, p-eIF 2α, eIF 2α, Chop and Actin were recorded by Western blotting bands. (B−H) Relative protein levels of p-PERK/PERK, p-IRE1α/IRE1α, ATF6/Actin, GRP 78/Actin, USP14/Actin, p-eIF 2α/eIF 2α and Chop/Actin in different groups were measured by Image J. The data are expressed as mean ± SD; (n = 4). $^{\#\#}P < 0.01$ *vs* NFD group; $^{*}P < 0.05$, $^{**}P < 0.01$ *vs* HFD group.

Studies have proven that the activity of AMPK is significantly inhibited in NAFLD mice, and the activation of AMPK can improve oxidative stress injury and lipid deposition [52, 53]. PGC-1α, a downstream molecule of AMPK, can regulate the expression of mitochondrial function-related genes to maintain mitochondrial function homeostasis [54, 55]. Some studies have confirmed that the activation of PGC-1α expression in liver cells improves energy metabolism [56, 57]. In the present study, ACR treatment obviously up-regulated the p-AMPKα and PGC-1α expressions, suggesting that ACR can activate the AMPK/PGC-1α pathway in HFD-fed mice to regulate energy metabolism. Collectively, these results indicate that ACR can enhance the activities of mitochondrial respiratory chain complexes, promote ATP synthesis, and improve energy metabolism in NAFLD mice through the activation of the AMPK/PGC-1α signaling pathway.

The pathogenesis of NAFLD involves intricate mechanisms of lipotoxicity, encompassing oxidative stress injury and ER stress induction [18]. Lipid accumulation triggers protein misfolding or unfolding in the ER, leading to the activation of the unfolded protein response (UPR). The UPR, mediated by GRP78, stimulates pathways involving PERK, ATF6, and IREα to regulate lipid metabolism [19, 20]. Thus, alleviating ER stress is a pivotal therapeutic approach in NAFLD manage-

ment. In our study, ACR inhibited the up-regulation of GRP78, p-PERK, p-IRE1α, ATF6, p-eIF2α, and Chop proteins, indicating its ability to alleviate HFD-induced ER stress. Moreover, USP14, which plays an important role in protein degradation by participating in the post-translational modification of proteins in the UPR system, was also investigated in our study. Studies have reported that the high expression of USP14 is correlated with fatty acid metabolism [43]. USP14 may decrease the level of TG in the development of NAFLD by regulating fatty acid metabolism [44]. Our findings demonstrated that ACR treatment reduced the expression level of USP14 in NAFLD mice. All these results highlight the potential of ACR to restore ER homeostasis and mitigate lipid accumulation in NAFLD.

However, our study has several limitations that should be acknowledged. Firstly, while we investigated the effects of ACR on a NAFLD mouse model and explored the preliminary mechanisms, we did not confirm the molecular mechanism specifically in hepatocytes. Future studies should aim to elucidate the underlying molecular pathways at the cellular level by isolating the total alkaloids. Secondly, ACR is a complex mixture of alkaloids, and further investigations are warranted to explore the integrated effects of ACR on the improvement of NAFLD. This can be achieved through comprehensive approaches such as transcriptomics, proteomics, metabolomics, and network pharmacology analysis [58]. Thirdly, our research primarily focused on oxidative stress, abnormal energy metabolism, and ER stress. Other critical mechanisms involved in NAFLD pathogenesis, such as inflammation and autophagy, were not explored in our study. Therefore, future investigations should encompass a broader range of mechanisms to fully elucidate the comprehensive therapeutic effects and underlying mechanisms of ACR in NAFLD.

Conclusion

In conclusion, this study represents the pioneering investigation into the effects and underlying mechanisms of ACR in ameliorating lipid accumulation in NAFLD. The findings of this study provide compelling evidence for the significant amelioration of hepatic steatosis and oxidative injury in HFD-induced NAFLD mice following ACR administration. These lipid-lowering effects are attributed to the enhancement of mitochondrial energy metabolism and suppression of ER stress. The results of this study highlight the potential of ACR as a therapeutic agent for NAFLD and warrant further comprehensive investigations in this field.

References

[1] Yan TT, Yan NN, Wang P, *et al*. Herbal drug discovery for the treatment of nonalcoholic fatty liver disease [J]. *Acta Pharm Sin B*, 2020, **10**(1): 3-18.

[2] Spearman CW, Afihene M, Betiku O, *et al*. Epidemiology, risk factors, social determinants of health, and current management for non-alcoholic fatty liver disease in sub-Saharan Africa [J]. *Lancet Gastroenterol Hepatol*, 2021, **6**(12): 1036-1046.

[3] Ginès P, Graupera L, Lammert F, *et al*. Screening for liver fibrosis in the general population: a call for action [J]. *Lancet Gastroenterol Hepatol*, 2016, **1**(3): 256-260.

[4] Li H, Meng Y, He SW, *et al*. Macrophages, chronic inflammation, and insulin resistance [J]. *Cells*, 2022, **11**(19): 3001.

[5] Suri J, Borja S, Lim JK. Combination strategies for pharmacologic treatment of non-alcoholic steatohepatitis [J]. *World J Gastroenterol*, 2022, **28**(35): 5129-5140.

[6] Shi YW, Fan JG. Current status and challenges in the drug treatment for fibrotic nonalcoholic steatohepatitis [J]. *Acta Pharmacol Sin*, 2022, **43**(5): 1191-1199.

[7] Negi CK, Babica P, Bajard L, *et al*. Insights into the molecular targets and emerging pharmacotherapeutic interventions for nonalcoholic fatty liver disease [J]. *Metabolism*, 2022, **126**: 154925.

[8] Mahata T, Sengar AS, Basak M, *et al*. Hepatic regulator of G protein signaling 6 (RGS6) drives non-alcoholic fatty liver disease by promoting oxidative stress and ATM-dependent cell death [J]. *Redox Biol*, 2021, **46**: 102105.

[9] Heida A, Gruben N, Catrysse L, *et al*. The hepatocyte IKK: NF-κB axis promotes liver steatosis by stimulating *de novo* lipogenesis and cholesterol synthesis [J]. *Mol Metab*, 2021, **54**: 101349.

[10] Videla LA, Valenzuela R. Perspectives in liver redox imbalance: toxicological and pharmacological aspects underlying iron overloading, nonalcoholic fatty liver disease, and thyroid hormone action [J]. *Biofactors*, 2022, **48**(2): 400-415.

[11] Bovi APD, Marciano F, Mandato C, *et al*. Oxidative stress in non-alcoholic fatty liver disease. An updated mini review [J]. *Front Med*, 2021, **8**: 595371.

[12] Jadhav S, Protchenko O, Li F, *et al*. Mitochondrial dysfunction in mouse livers depleted of iron chaperone PCBP1 [J]. *Free Radic Biol Med*, 2021, **175**: 18-27.

[13] Peng KY, Watt MJ, Rensen S, *et al*. Mitochondrial dysfunction-related lipid changes occur in nonalcoholic fatty liver disease progression [J]. *J Lipid Res*, 2018, **59**(10): 1977-1986.

[14] Tang C, Kong LY, Shan MY, *et al*. Protective and ameliorating effects of probiotics against diet-induced obesity: a review [J]. *Food Res Int*, 2021, **147**: 110490.

[15] Polla D, Edmondson AC, Duvet S, *et al*. Bi-allelic variants in the ER quality-control mannosidase gene EDEM3 cause a congenital disorder of glycosylation [J]. *Am J Hum Genet*, 2021, **108**(7): 1342-1349.

[16] Barger SR, Penfield L, Bahmanyar S. Coupling lipid synthesis with nuclear envelope remodeling [J]. *Trends Biochem Sci*, 2021, **47**(1): 52-65.

[17] Kumar V, Xin XF, Ma JY, *et al*. Therapeutic targets, novel drugs, and delivery systems for diabetes associated NAFLD and liver fibrosis [J]. *Adv Drug Deliv Rev*, 2021, **176**: 113888.

[18] Flessa CM, Kyrou I, Nasiri-Ansari N, *et al*. Endoplasmic reticulum stress and autophagy in the pathogenesis of non-alcoholic fatty liver disease (NAFLD): current evidence and perspectives [J]. *Curr Obes Rep*, 2021, **10**(2): 134-161.

[19] Marciniak SJ, Chambers JE, Ron D. Pharmacological targeting of endoplasmic reticulum stress in disease [J]. *Nat Rev Drug Discov*, 2022, **21**(2): 115-140.

[20] Wu JC, Qiao S, Xiang YE, *et al*. Endoplasmic reticulum stress: multiple regulatory roles in hepatocellular carcinoma [J]. *Biomed Pharmacother*, 2021, **142**: 112005.

[21] Lin CJ, Chen CH, Liu FW, *et al*. Inhibition of intestinal glucose uptake by aporphines and secoaporphines [J]. *Life Sci*, 2006, **79**(2): 144-153.

[22] Wang FX, Zhu N, Zhou F, *et al*. Natural aporphine alkaloids with potential to impact metabolic syndrome [J]. *Molecules*, 2021, **26**(20): 6117.

[23] Zhu ZL, Li W. Study of effect of total alkaloids extracts of Lotus Leaf on the lipids of hyperlipemia rats [J]. *Heilongjiang Medi J*, 2010, **23**(3): 363-364.

[24] Adjoumani JJY, Wang K, Zhou M, *et al*. Effect of dietary betaine on growth performance, anti-oxidant capacity and lipid metabolism in blunt snout bream fed a high-fat diet [J]. *Fish Physiol Biochem*, 2017, **43**(6): 1733-1745.

[25] He JY, Zhu S, Goda Y, *et al*. Quality evaluation of medicinally-used Codonopsis species and Codonopsis Radix based on the contents of pyrrolidine alkaloids, phenylpropanoid and polyacetylenes [J]. *J Nat Med*, 2014, **68**(2): 326-339.

[26] He JY, Zhu S, Komatsu K, *et al*. Genetic polymorphism of medicinally-used Codonopsis species in an internal transcribed

spacer sequence of nuclear ribosomal DNA and its application to authenticate Codonopsis Radix [J]. *J Nat Med*, 2014, **68**(1): 112-124.
[27] Li CY, Xu HX, Han QB, *et al*. Quality assessment of Radix Codonopsis by quantitative nuclear magnetic resonance [J]. *J Chromatogr A*, 2009, **1216**(11): 2124-2129.
[28] Deng XL, Fu YJ, Luo S, *et al*. Polysaccharide from Radix Codonopsis has beneficial effects on the maintenance of T-cell balance in mice [J]. *Biomed Pharmacother*, 2019, **112**: 108682.
[29] Luan F, Ji YF, Peng LX, *et al*. Extraction, purification, structural characteristics and biological properties of the polysaccharides from Codonopsis pilosula: a review [J]. *Carbohydr Polym*, 2021, **261**: 117863.
[30] Wang JN, Wang CD, Kan LT, *et al*. Herbal extract from *Codonopsis pilosula* (Franch.) Nannf. enhances cardiogenic differentiation and improves the function of infarcted rat hearts [J]. *Life*, 2021, **11**(5): 422.
[31] Bai RB, Li WY, Li YD, *et al*. Cytotoxicity of two water-soluble polysaccharides from *Codonopsis pilosula* Nannf. var. modesta (Nannf.) L. T. Shen against human hepatocellular carcinoma HepG2 cells and its mechanism [J]. *Int J Biol Macromol*, 2018, **120**: 1544-1550.
[32] Liu W, Lv X, Huang WH, *et al*. Characterization and hypoglycemic effect of a neutral polysaccharide extracted from the residue of *Codonopsis pilosula* [J]. *Carbohydr Polym*, 2018, **197**: 215-226.
[33] Chu X, Liu XJ, Qiu JM, *et al*. Effects of Astragalus and *Codonopsis pilosula* polysaccharides on alveolar macrophage phagocytosis and inflammation in chronic obstructive pulmonary disease mice exposed to PM2.5 [J]. *Environ Toxicol Pharmacol*, 2016, **48**: 76-84.
[34] Meng Y, Xu YJ, Chang C, *et al*. Extraction, characterization and anti-inflammatory activities of an inulin-type fructan from *Codonopsis pilosula* [J]. *Int J Biol Macromol*, 2020, **163**: 1677-1686.
[35] Jiang YP, Liu YF, Guo QL, *et al*. Sesquiterpene glycosides from the roots of *Codonopsis pilosula* [J]. *Acta Pharm Sin B*, 2016, **6**(1): 46-54.
[36] Liu J, Tang T, Wang GD, *et al*. LncRNA-H19 promotes hepatic lipogenesis by directly regulating miR-130a/PPARγ axis in non-alcoholic fatty liver disease [J]. *Biosci Rep*, 2019, **39**(7): BSR20181722.
[37] Su DX, Zhang RF, Zhang CL, *et al*. Phenolic-rich lychee (*Litchi chinensis* Sonn.) pulp extracts offer hepatoprotection against restraintstress-induced liver injury in mice by modulating mitochondrial dysfunction [J]. *Food Funct*, 2016, **7**: 508-515.
[38] Che Y, Wang ZP, Yuan Y, *et al*. Role of autophagy in a model of obesity: a long-term high fat diet induces cardiac dysfunction [J]. *Mol Med Rep*, 2018, **18**(3): 3251-3261.
[39] Ma YL, Brown PM, Lin DD, *et al*. 17-Beta hydroxysteroid dehydrogenase 13 deficiency does not protect mice from obesogenic diet injury [J]. *Hepatology*, 2021, **73**(5): 1701-1716.
[40] Willis SA, Bawden SJ, Malaikah S, *et al*. The role of hepatic lipid composition in obesity-related metabolic disease [J]. *Liver Int*, 2021, **41**(12): 2819-2835.
[41] Jiang X, Tan HY, Teng SS, *et al*. The role of AMP-activated protein kinase as a potential target of treatment of hepatocellular carcinoma [J]. *Cancers*, 2019, **11**(5): 647.
[42] Sun JC, Liu XZ, Shen CA, *et al*. Adiponectin receptor agonist AdipoRon blocks skin inflamm-ageing by regulating mitochondrial dynamics [J]. *Cell Prolif*, 2021, **54**(12): e13155.
[43] Liu B, Jiang SW, Li M, *et al*. Proteome-wide analysis of USP14 substrates revealed its role in hepatosteatosis *via* stabilization of FASN [J]. *Nat Commun*, 2018, **9**(1): 4770.
[44] Liu B, Zhang ZJ, Hu YY, *et al*. Sustained ER stress promotes hyperglycemia by increasing glucagon action through the deubiquitinating enzyme USP14 [J]. *Proc Natl Acad Sci USA*, 2019, **116**(43): 21732-21738.
[45] Negi CK, Babica P, Bajard L, *et al*. Insights into the molecular targets and emerging pharmacotherapeutic interventions for nonalcoholic fatty liver disease [J]. *Metabolism*, 2022, **126**: 154925.
[46] Liu YL, Zhang QZ, Wang YR, *et al*. Astragaloside IV improves high-fat diet-induced hepatic steatosis in nonalcoholic fatty liver disease rats by regulating inflammatory factors level via TLR4/NF-κB signaling pathway [J]. *Front Pharmacol*, 2021, **11**: 605064.
[47] Sun NN, Shen CP, Zhang L, *et al*. Hepatic Krüppel-like factor 16 (KLF16) targets PPARα to improve steatohepatitis and insulin resistance [J]. *Gut*, 2021, **70**(11): 2183-2195.
[48] Yuan GS, Yang ST, Liu M, *et al*. RGS12 is required for the maintenance of mitochondrial function during skeletal development [J]. *Cell Discov*, 2020, **6**: 59.
[49] Li SY, Li X, Chen FY, *et al*. Nobiletin mitigates hepatocytes death, liver inflammation, and fibrosis in a murine model of NASH through modulating hepatic oxidative stress and mitochondrial dysfunction [J]. *J Nutr Biochem*, 2022, **100**: 108888.
[50] Alghamdi F, Alshuweishi Y, Salt IP. Regulation of nutrient uptake by AMP-activated protein kinase [J]. *Cellular Signal*, 2020, **76**: 109807.
[51] Trefts E, Shaw RJ. AMPK: restoring metabolic homeostasis over space and time [J]. *Mol Cell*, 2021, **81**(18): 3677-3690.
[52] Zhang Y, Wang RQ, Yao HJ, *et al*. Mangiferin ameliorates HFD-Induced NAFLD through regulation of the AMPK and NLRP3 inflammasome signal pathways [J]. *J Immunol Res*, 2021, **2021**: 4084566.
[53] Loeffelholz CV, Coldewey SM, Birkenfeld AL. A narrative review on the role of AMPK on *de novo* lipogenesis in non-alcoholic fatty liver disease: evidence from human studies [J]. *Cells*, 2021, **10**(7): 1822.
[54] Liu JX, Wang YT, Lin LG. Small molecules for fat combustion: targeting obesity [J]. *Acta Pharm Sin B*, 2019, **9**(2): 220-236.
[55] Ryu JY, Choi HM, Yang H, *et al*. Dysregulated autophagy mediates sarcopenic obesity and its complications *via* AMPK and PGC1α signaling pathways: potential involvement of gut dysbiosis as a pathological link [J]. *Int J Mol Sci*, 2020, **21**(18): 6887.
[56] Lee Y, Lee J, Lee M, *et al*. *Chrysanthemum morifolium* flower extract ameliorates obesity-induced inflammation and increases the muscle mitochondria content and AMPK/SIRT1 activities in obese rats [J]. *Nutrients*, 2021, **13**(10): 3660.
[57] Xu FB, Li YF, Cao Z, *et al*. AFB-induced mice liver injury involves mitochondrial dysfunction mediated by mitochondrial biogenesis inhibition [J]. *Ecotoxicol Environ Saf*, 2021, **216**: 112213.
[58] Guo R, Luo XL, Liu JJ, *et al*. Omics strategies decipher therapeutic discoveries of traditional Chinese medicine against different diseases at multiple layers molecular-level [J]. *Pharmacol Res*, 2020, **152**: 104627.

Cite this article as: FAN Cailian, WANG Guan, CHEN Miao, LI Yao, TANG Xiyang, DAI Yi. Therapeutic potential of alkaloid extract from Codonopsis Radix in alleviating hepatic lipid accumulation: insights into mitochondrial energy metabolism and endoplasmic reticulum stress regulation in NAFLD mice [J]. *Chin J Nat Med*, 2023, **21**(6): 411-422.